Inorg. Chem. **2003**, *42*, 3715–3717

Speciation and Unusual Reactivity in PuO_{2+x}

Steven D. Conradson,*,† Bruce D. Begg,‡ David L. Clark,† Christophe Den Auwer,§ Francisco J. Espinosa-Faller,† Pamela L. Gordon,† Nancy J. Hess,|| Ryan Hess,† D. Webster Keogh,† Luis A. Morales,† Mary P. Neu,† Wolfgang Runde,† C. Drew Tait,† D. Kirk Veirs,† and Phillip M. Villella†

Los Alamos National Laboratory, Los Alamos, New Mexico 87545, ANSTO, Menai, NSW 2234, Australia, CEA Marcoule, 30207 Bagnols sur Ceze Cedex, France, and Pacific Northwest National Laboratory, Richland, Washington 99352

Received September 18, 2002

Pu L_3 XAFS measurements show that the excess oxygen in single phase PuO_{2+x} occurs as oxo groups with Pu–O distances of 1.83–1.91 Å. This distance and the energy of the edge (via comparison with a large number of related compounds) are more consistent with a Pu(IV/V) than a Pu(IV/VI) mixture. Analogous to Pu(IV) colloids, although the Pu–Pu pair distribution remains single site even when it shows substantial disorder, the Pu–O distribution can display a number of additional shells at specific distances up to 3.4 Å even in high fired materials when no oxo groups are present, implying intrinsic $H^+/OH^-(/H_2O)$. The number of oxo atoms increases when samples are equilibrated with humid air at ambient temperature, indicating that the Pu reactivity in this solid system differs notably from that of isolated complexes and demonstrating the importance of nanoscale cooperative phenomena and total free energy in determining its chemical properties.

The chemistry of PuO_2, a compound central to environmental remediation and waste dispostion, was recently complicated by the report of PuO_{2+x}. The excess O atoms of PuO_{2+x} were posited as interstitial in tandem with Pu(VI) sites[1] on the basis of photoemission[2] and by analogy with crystallographic studies of UO_{2+x}.[3] XAFS measurements described here demonstrate their occurrence as Pu(V) oxo moieties as well as additional Pu−O distances indicative of intrinsic H_2O hydrolysis products in the lattice. These are found in almost all samples of ostensibly pure PuO_2 and can apparently promote further oxidation of Pu(IV) by H_2O, perhaps via stabilization as nondiffracting nanoscale domains within the host lattice.

Ordered PuO_2 (**cd**) was produced via the decomposition in air of finely ground KPu_2Se_6. High (**a**) and low fired PuO_2 were synthesized by firing Pu metal in air at 1000 and 800 °C, respectively. PuO_{2+x} with $x = 0.17$ ($a = 5.4022$ Å) and 0.26 ($a = 5.4038$ Å) was made by reacting the high fired PuO_2 (**a**) with H_2O vapor at 300 °C, with x determined from the H_2 generated by the reaction. A second high fired PuO_2 (**b**) was equilibrated for two weeks above 65, 51, and 15 wt % H_2SO_4 (15%, 37%, and 80% humidity). The ambient temperature oxidation sample (**mo**) was prepared by the complete oxidation of a δ PuGa chip with H_2O vapor catalyzed by 0.05 Torr of HCl and was single phase with broad peaks. Pu L_3 XAFS spectra were measured at 80 K on SSRL beamline 4-2 using a Ge detector.[4] Calibration, normalization, background subtraction, and curve-fitting were done similarly for all spectra. $k^3\chi(k)$ were fit from 3.1 to 14.4 $Å^{-1}$, with the ΔE_0s, σs, and total numbers of O atoms constrained over narrow ranges. R and N ranges for the oxo shell were derived from curve-fits of both data and Fourier filters using different constraints and from ratioing[5] (Table 1). The accuracy of the energies of the spectral features (Table 2) is $\pm 0.5-1.0$ eV.

Dozens of phase pure (by diffraction) samples of PuO_2 from many sources have produced a very diverse set of EXAFS spectra (Figure 1 portrays five) indicative of a correspondingly wide range of Pu−O bonding modes and composite local structures. The common features are the positions of the single Pu contribution at $R - ø = 3.75$ Å and primary O contribution at ∼1.9 Å. Consistent with diffraction, the average Pu sublattice is retained, although the diminished amplitude of the Pu peak in $\chi(R)$ indicates that the Pu shell can be highly disordered. In contrast, a

* To whom correspondence should be addresed. E-mail: conradson@lanl.gov.
† Los Alamos National Laboratory.
‡ ANSTO.
§ CEA Marcoule.
|| Pacific Northwest National Laboratory.

(1) Haschke, J. M.; Allen, T. H.; Morales, L. A. *Science* **2000**, *237*, 285.
(2) Stakebake, J. L.; Larson, D. T.; Haschke, J. M. *J. Alloys Compd.* **1993**, *202*, 251.
(3) Park, K.; Olander, D. R. *High Temp. Sci.* **1990**, *29*, 203. Willis, B. T. M. *J. Chem. Soc., Faraday Trans. 2* **1987**, *83*, 1073. Matzke, H. *J. Nucl. Mater.* **1983**, *114*, 121.
(4) A more complete description of current experimental and analytical procedures can be found in, e.g.: Espinosa, F. J.; Villella, P.; Lashley, J. C.; Conradson, S. D.; Cox, L. E.; Martinez, R.; Martinez, B.; Morales, L.; Terry, J.; Pereyra, R. A. *Phys. Rev.* **2001**, *B63*, 4111.
(5) Teo, B.-K. *EXAFS: Basic Principles and Data Analysis*; Springer-Verlag: New York, 1986.

10.1021/ic026044l CCC: $25.00
Published on Web 05/20/2003

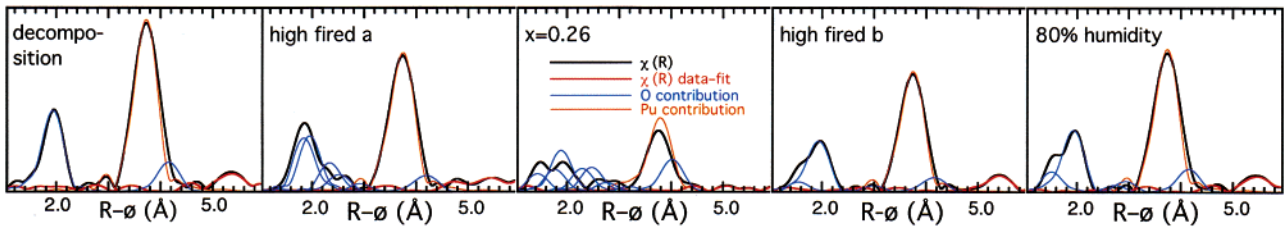

Figure 1. Fourier transform moduli of data, data-fit, and contributions of individual shells, showing the range of local structures exhibited by PuO_{2+x}.

Table 1. Selected Pu−O/Pu Metrical Parameters for 10 Samples

sample (cryst struct)	O (1.8−1.9 Å) *R* (Å)/N	O (2.2 < *R* < 3.8 Å) *R* (Å) for 6 shells			Pu *R* (Å)	O (at 4.5 Å) *R* (Å)
		2.336			3.816	4.474
PuO_2 (**cd**)		2.34			3.83	4.53
high fired (**a**)	na−1.94	2.25	2.36	2.75	3.84	4.57
	0−0.20	2.95	3.30			
$x = 0.17$	1.86−1.91	2.26	2.36		3.84	4.55
	0.12−0.26		3.30			
$x = 0.26$	1.83−1.87	2.22	2.34	2.75	3.85	4.42
	0.51−0.56	2.92	3.19	3.63		
ambient *T* oxdn (**mo**)	1.84−1.87	2.21	2.34	2.79	3.82	4.45
	0.24−0.31	2.96	3.26	3.55		
low fired	1.81−1.84	2.28	2.39	2.89	3.83	4.55
	0.21−0.34	3.06	3.32			
high fired (**b**)	1.91		2.35	2.84	3.84	4.54
	0.15−0.35	3.11	3.36			
15% humidity	1.89		2.34		3.84	4.54
	0.18−0.31	3.12	3.34			
37% humidity	1.89−1.90	2.30	2.39	2.89	3.84	4.55
	0.26−0.51	3.09	3.34			
80% humidity	1.88−1.89		2.34		3.83	4.53
	0.30−0.57	3.11	3.33			

Table 2. XANES Parameters: Edge Inflection Point of Ordered PuO_2 = 18062.3 eV on the Basis of First Inflection Point of Zr Metal = 17999.35

sample	IP energy	ΔPuO_2	peak energy	height
Pu(0) metal	18057.0	−5.3	18067.3	na
Pu(III) aquo	18060.0	−2.3	18064.3	1.85
Pu(IV) aquo	18063.2	0.9	18068.7	1.72
Pu(V) aquo	18062.3	0.0	18067.6	1.43
Pu(VI) aquo	18064.9	2.6	18069.5	1.47
Pu(III) zrcnlt[10]	18059.1	−3.1	18064.8	1.62
Pu(IV) zrcnlt[9]	18062.9	0.6	18069.1	1.71
Pu(IV) glass[9]	18063.2	0.9	18069.4	1.66
$PuCl_3$	18059.2	−3.1	18064.7	1.43
$(Et_4N)_2PuCl_6$	18061.4	−0.9	18068.1	1.52
Pu(IV) colloids	18063.2 ± 0.8	0.5−1.2	18068.7	1.5−1.7
Pu(IV)(NO_3)	18063.9	1.6	18068.5	1.85
Pu(IV)(CO_3)	18063.9	1.6	18068.5	1.78
$PuO_2(CO_3)_3^{5-}$	18062.9	0.6	18067.2	1.46
$PuO_2(CO_3)_3^{4-}$	18064.7	2.4	18069.7	1.43
$PuO_2(OH)_4^{2-}$	18063.9	1.6	18069.3	1.44
PuS_2	18058.0	−4.3	18064.0	1.34
PuO_2 (**cd**)	18062.3 ± 0.3	reference	18068.6 ± 0.3	1.55
high fired (**a**)	18062.2	−0.1	18068.8	1.50
$x = 0.17$	18063.1	0.8	18069.8	1.45
$x = 0.26$	18061.6	−0.7	18068.6	1.43
ambient temp oxdn	18062.7	0.4	18069.5	1.42
low fired	18062.2	−0.1	18068.9	1.45
high fired (**b**)	18061.2	−1.1	18068.2	1.39
15% humidity	18062.0	−0.3	18068.6	1.46
37% humidity	18062.4	0.1	18068.6	1.53
80% humidity	18062.2	−0.1	18068.7	1.47

multisite O contribution is demonstrated by additional shoulders and resolved peaks both below and, especially in the spectra of the materials involved in the ambient and 300 °C oxidations, above the main O peak, the amplitude of which decreases with increasing spectral and structural complexity.

These observations are corroborated by the curve-fitting results (Figure 1 and Table 1). All of the features of the **cd** spectrum are well fit using only the crystallographic radial distribution function,[6] with errors for the nearest O and Pu shells of <0.02 Å. However, good fits of the complicated spectra of the other samples are obtained only by introducing additional O shells and, for many samples, large Pu Debye-Waller factors. The most significant O shell is the one containing a fraction of an atom at 1.8−1.9 Å. This distance corresponds to oxo groups associated with Pu(≥V). Although this length implies Pu(V), the *x*/oxo ratio of ca. 0.5 and maximum *x* of 0.25 suggest Pu(VI) if H^+ is absent. The salient characteristic of the other shells is their distance, which, unlike N and σ, is minimally correlated with nearby shells in the curve-fits.

The Pu−O distances >2.5 Å (Table 1), which have been ascribed to specific moieties such as Pu−OH in the colloids,[7] appear correlated. The **a** and **mo** samples show significant numbers of O atoms near 2.76, 2.94, 3.26, and 3.6 Å in addition to the oxo group near 1.86 Å. In contrast, the **b** samples have marginally significant shells near 2.87, 3.11, and 3.34 Å in addition to their oxo group near 1.90 Å. As observed in the raw data as well as the fitting results, these characteristics of the starting material are unchanged after the reaction of high fired **b** with H_2O.

In order to use the X-ray absorption near edge spectra (XANES) (Figure 2 and Table 2) to determine the valence,[7,8] the parameters affecting the edge energy (the inflection point of the primary absorption increase) must be evaluated. On the basis of the table, in order of importance, these would be (1) the Pu valence, (2) the types of ligands, and (3) disorder. The shift relative to PuO_2 can then be estimated by summing these factors and multiplying by the fraction of Pu(V) or Pu(VI). In common with Np and Am, the covalency of the oxo groups results in a shift in edge energy for Pu(IV) → (V) of around −1.0 eV. The (IV−VI) difference is +0.8−1.7 eV. Enhanced charge donation by O^{2-} (PuO_2) and OH^- ($PuO_2(OH)_4^{2-}$) results in a −0.9 eV change relative to aquo complexes. (Even larger shifts occur with Cl^- and S^{2-}.) The spectra from the zirconolite, glass, two sets of PuO_{2+x} samples, and colloids suggest that disorder can alter the energy by +0.5−1.0 eV.

(6) Gardner, E. R.; Markin, T. L.; Street, R. S. *J. Inorg. Nucl. Chem.* **1965**, *27*, 541.
(7) Conradson, S. D. *Appl. Spectrosc.* **1998**, *52*, A252.
(8) Allen, P. G.; Shuh, D. K.; Bucher, J. J.; Edelstein, N. M.; Reich, T.; Denecke, M. A.; Nitsche, H. *J. Phys. IV* **1997**, *7*, 789. Conradson, S. D.; Al Mahamid, I.; Clark, D. L.; Hess, N. J.; Hudson, E. A.; Neu, M. P.; Palmer, P. D.; Runde, W. H.; Tait, C. D. *Polyhedron* **1998**, *17*, 599. Antonio, M. R.; Soderholm, L.; Williams, C. W.; Blaudeau, J. P.; Bursten, B. E. *Radiochim. Acta* **2001**, *89*, 17.

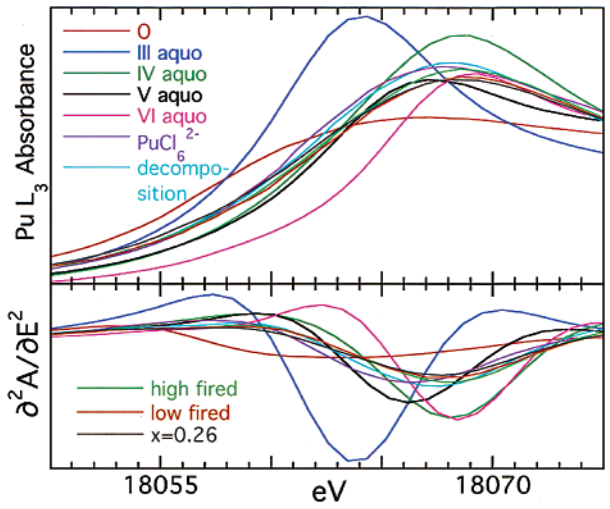

Figure 2. Normalized XANES spectra of 10 representative samples.

Using these values and the EXAFS results, the energies should be higher than that of PuO_2 by ~0.7 eV for the **a** and ~0.4 eV for the more ordered **b** samples. These would increase to, respectively, ~1.0 and ~0.7 eV for 25% Pu(VI). In contrast, the observed shifts relative to the edge of PuO_2 are 0.1 ± 0.5 for **a** and −0.5 ± 0.4 eV for **b**. This evaluation shows that the energies of the PuO_{2+x} spectra are close to or less than that of PuO_2 and well below those of the colloids and are thus more consistent with a Pu(IV/V) than Pu(V/VI) mixture or even pure Pu(IV). The lower energy of the **b** samples relative to **a** may reflect fewer H^+ and less disorder in the **b** lattice, consistent with their smaller numbers of Pu−O pairs at >2.5 Å.

These results indicate that the excess O in PuO_2 occurs as localized Pu(V)−oxo moieties. Together with H^+/OH^-(/H_2O), these subsequently induce highly specific sets of additional O displacements. This process is directly analogous to the situation in hydrous PuO_2.[7] The narrow ranges for the other Pu−O distances suggest that a better description than "disordered" would be that the oxygen excess in combination with H_2O creates PuO_2-type compounds that are "differently" ordered. The quite similar diffraction patterns and very narrow range of Pu−Pu distances demonstrate that the average Pu sublattice is conserved. One way that >20% of the cation sites can be occupied by Pu atoms with a radically different coordination geometry from the cubic host is as nondiffracting, serpentine networks.[9] Two-state entropy contributions could then stabilize nanoscale phase separation into PuO_2 intimately associated with, e.g., ordered, oligomeric $Pu_{4-x}O_{13}H_{6+4x}$ domains if the latter can be structured to conserve the density and minimize the interfacial strain. The resultant total free energy of the nanoscale heterogeneous compound would then explain the observation that H_2O vapor at ambient temperature oxidizes Pu(IV) to Pu(V), a reaction that does not occur with mononuclear Pu(IV). This unusual stability also implies that, contrary to the expectation from the behavior of pure materials, the higher valence Pu in PuO_{2+x} may not have higher solubility than the bulk solid.

Acknowledgment. This work was supported by DOE DP and OBES Division of Chemical Sciences under Contract W-7405. XAFS measurements were performed at the Stanford Synchrotron Radiation Laboratory which is supported by DOE OBES. Health physics operations at SSRL were supported by the Seaborg Institute at LANL.

Supporting Information Available: Figures of $\chi(k)$ and $\chi(R)$ data and fits and XANES for all listed compounds. This material is available free of charge via the Internet at http://pubs.acs.org.

IC026044L

(9) Conradson, S. D. Unpublished results.
(10) zrclnt = $Ca_{0.2}Pu_{0.2}HfTi_{1.6}Al_{0.4}O_7$, annealed in 3.5%$H_2$ in N_2 (III) and air (IV); glass = Pu(IV) in borosilicate glass.